Published in final edited form as:
Biomaterials. 2011 November ; 32(33): 8676–8683. doi:10.1016/j.biomaterials.2011.07.072.

Enhanced Osseointegration of Titanium Implant Through the Local Delivery of Transcription Factor SATB2

S.G. Yan[1,2,3,+], **J. Zhang**[1,2,3,+], **Q.S. Tu**[1], **J.H. Ye**[1,4], **E. Luo**[1,5], **M. Schuler**[6], **M.S. Kim**[1], **T. Griffin**[7], **J. Zhao**[1,8], **X.J. Duan**[1,2], **DL Cochran**[9], **D. Murray**[1], **P.S. Yang**[2,3,*], and **J. Chen**[1,*]

S.G. Yan: figure1911@hotmail.com; J. Zhang: teadenzj@sdu.edu.cn; Q.S. Tu: qisheng.tu@tufts.edu; J.H. Ye: yjh98001@163.com; E. Luo: En.Luo@tufts.edu; M. Schuler: martin.schuler@straumann.com; M.S. Kim: Min_Seok.Kim@tufts.edu; T. Griffin: terrence.griffin@tufts.edu; J. Zhao: yuzj_260@hotmail.com; X.J. Duan: miqiu410@yahoo.com.cn; DL Cochran: cochran@uthscsa.edu; D. Murray: Dana.murray@tufts.edu; P.S. Yang: yangps@sdu.edu.cn; J. Chen: jk.chen@tufts.edu

[1]Division of Oral Biology, Department of General Dentistry, Tufts University School of Dental Medicine, One Kneeland Street, Boston, MA 02111, USA. Tel: 617-636-0341; Fax: 617-636-0878 [2]School of Stomatology, Shandong University, 44 West Wenhua Road, Jinan, Shandong Province 250012, China. Tel: +86-531-88382368; Fax: +86-531-82950194 [3]Shandong Provincial Key Lab of Oral Biomedicine, Jinan, Shandong Province 250012, China. Tel: +86-531-88382769; Fax: +86-531-82950194 [4]Institute of Stomatology, School of Stomatology, Nanjing Medical University, Nanjing, Jiangsu Province, China [5]Department of Oral and Maxillofacial Surgery, School of Stomatology, Sichuan University, Chengdu, China [6]Institute Straumann AG, Basel, Switzerland [7]Department of Periodontics, Tufts University School of Dental Medicine, One Kneeland Street, Boston, MA 02111, USA. Tel: 617-636-6530; Fax: 617-636-0911 [8]Department of Oral and Maxillofacial Surgery, Ninth People's Hospital Affiliated to Shanghai Jiao Tong University, School of Medicine, Shanghai Key Laboratory of Stomatology, Shanghai, China [9]Department of Periodontics, University of Texas Health Science Center at San Antonio, TX, USA. Tel: 21-567-3602

Abstract

Titanium implants are widely used in dentistry and orthopaedic surgery. Nevertheless, bone regeneration around the implant is a relatively slow process, after placement. This study assessed whether SATB2 can enhance osseointegration of a titanium implant. To determine the effect of SATB2 in implant integration, two different viruses encoding SATB2 (PBABE-Satb2 virus or RCAS-Satb2 virus) were locally administered to the bone defect prior to titanium implant placement in our established transgenic TVA mice. Seven and 21 days post implantation, the femurs were isolated for quantitative real-time RT-PCR, H&E staining, immunohistochemical (IHC) staining, and microcomputed tomography (microCT) analysis. Quantitative real-time RT-PCR results demonstrated that the *in vivo* overexpression of SATB2 enhanced expression levels of potent osteogenic transcription factors and bone matrix proteins. We also found that 21 days after implantation, there were no significant differences in the expression levels of SATB2, Osx,

[*]Correspondence to Jake Chen and Pi-Shan Yang: Jake (Jinkun) Chen, D.D,S., Ph.D., Division of Oral Biology, Tufts University School of Dental Medicine, 1 Kneeland Street, Boston, MA, 02111, USA, Tel: 617-636-2729; Fax: 617-636-0878, jk.chen@tufts.edu and Pishan Yang, D.D.S., Ph.D., School of StomatologyShandong University, 44 West Wen Hua Road, Jinan, Shandong Province 250012, P. R. of China, Tel: +86-531-88382368; Fax: +86-531-82950194, yangps@sdu.edu.cn.
[+]These two authors contribute to this work equally.

Runx2, COLI, OC, and BSP between the RCAS-Satb2 group and the RCAS group. Histological analysis showed that SATB2 overexpression significantly enhanced new bone formation and bone-to-implant contact after implantation. IHC staining analysis revealed that forced expression of SATB2 increased the number of BSP-positive cells surrounding the implant. MicroCT analysis demonstrated that *in vivo* overexpression of SATB2 significantly increased the density of the newly formed bone surrounding the implant. These results conclude that *in vivo* overexpression of SATB2 significantly accelerates osseointegration of titanium implants and SATB2 can serve as a potent molecule in promoting tissue regeneration.

Keywords

implant; SATB2; osseointegration; TVA mice

1. Introduction

In oral health care, the use of dental implants has become a routine procedure. Osseointegration, or direct bone-to-implant contact (BIC), plays an important role in the biological and clinical success of established dental implants[1, 2]. To improve and even accelerate the process of osseointegration, various studies on implant material and bone regeneration have been undertaken. For example, much effort has been made to modify the surface properties of the titanium dental implants to facilitate osseointegration [3–6]. Moreover, bioactive molecules, such as platelet-released growth factors (PRGF), transforming growth factors (TGF), and bone morphogenetic proteins (BMPs), were used to coat the dental implants to improve the BIC[7–9]. Systemic administration of bone-regulating hormones, such as calcitonin, parathyroid hormone, and estrogen, found to significantly improve the implants anchorage in osteoporotic rats [10–12]. Local administration of a potent osteogenic transcription factor, Osterix, via a retroviral delivery system also significantly accelerated osseointegration of the implant [13].

Although researchers have made significant achievements in improving osseointegration after dental implantation, currently the mechanism of osseointegration at the dental implant surface is still not clear, and in some clinical circumstances, accelerated establishment of osseointegration is required to fulfill the urgent need of function restoration. Based on the fact that osseointegration of dental implants is achieved by the osteogenic activity of osteoblasts, enhancing the recruitment and differentiation of osteoprogenitor cells is the key in accelerating BIC.

Special AT-rich sequence-binding protein 2 (SATB2) is a nuclear matrix protein that has a pivotal role in craniofacial development and osteoblast differentiation [14]. SATB2 binds to the nuclear matrix-attachment regions (MARs) and activates gene transcription in aMAR-dependent manner [15]. *Satb2* gene knockout mice exhibit multiple craniofacial defects including a significant truncation of the mandible, a shortening of the oral maxillofacial bones, and the defects in osteoblast differentiation and function [14, 16]. SATB2 was also found to modulate the osteogenic activity of other essential osteogenic transcriptional factors such as Runx2 and activating transcription factor 4 (ATF4), and directly enhance the expressions of bone marker genes such as bone sialoprotein (BSP) and osteocalcin (OC) [14]. In 2009, Savarese et al. reported that both SATB1 and SATB2 bind to the *Nanog* locus *in vivo* and regulate *Nanog* gene expression and embryonic stem (ES) cell pluripotency[17]. Taken together, these previous findings indicate that SATB2 acts as a master gene regulating osteoblast differentiation and plays an important role in the development of craniofacial and dental structures.

In this study, local overexpression of SATB2 was achieved *in vivo* using two different retroviral gene delivery systems to explore the effect of SATB2 on host responses after implantation. The role of SATB2 in regulating osteogenic differentiation and bone regeneration at the bone-implant interface was also investigated to evaluate the potential of clinical application of this potent transcription factor in promoting bone-to-implant contact.

2. Materials & Methods

2.1 Plasmids

The mouse *Satb2* cDNA was released from pBs-SK-*Satb2* (a gift from Dr. Grosschedl, Gene Center and Institute of Biochemistry, University of Munich, Germany), and was ligated into the *BamH*I/*Eco*RI sites of a retroviral vector, pBABE-hygro (ID: 1765, Addgene Inc., Cambridge, MA), creating the plasmid pBABE-*Satb2*. To produce an RCAS virus encoding the *Satb2* gene, *Satb2* cDNA was cloned into the ClaI site of RCASBP (A) (a gift from Dr. Stephen Hughes, National Cancer Institute Frederick Cancer Research and Development Center) through the Cla12-Nco shuttle vector. The resulted RCAS viral vector encoding *Satb2* was named as RCAS-*Satb2*.

2.2 Production of high-titer pBABE or RCAS viral stocks

The retroviral vectors, pBABE-*Satb2* and pBABE-hygro, were transfected into HEK-293T cells using Lipofectamine transfection reagent (Invitrogen, Carlsbad, CA). Forty-eight hours after the transfection, the supernatant was collected, filtered through a 0.45 μm filter (Millipore, Bedford, MA), and mixed with 40% PEG-8000 in PBS to reach a final concentration of 12% (Sigma-Aldrich Corporation, St. Louis, MO). After incubated in ice for at least 12 hours, the virus-PEG8000 mixtures were centrifuged at 4000 rpm (4°C) for 10 minutes. The pellets were dissolved in DMEM to achieve a viral titer of 10^8 cfu/ml. The RCAS vectors, RCAS-*Satb2* and RCASBP(A), were prepared as previously described [18]. The viral supernatant was centrifuged at 26,000 rpm (4°C) for 2.5 hours. The pellets were re-suspended to achieve a viral titer of 10^8 cfu/ml.

2.3 Animal surgery and the application of viral stocks

The animals used in our *in vivo* experiments were 10-week-old BSP/TVA transgenic mice [19]. These transgenic mice were generated in which TVA, an 800 bp avian retroviral receptor for subgroup-A avian aleukosis virus, was driven by a 4.9 kb mouse BSP promoter. Therefore, in BSP/TVA mice, only BSP-expressing bone-forming cells are susceptible to the infection with a replication-competent, subgroup A avian leucosis viral (ASLV) vector, RCAS, which makes this transgenic mouse line an ideal model for the study of bone tissue regeneration under the influence of certain regulatory factors. The animals were maintained and used in accordance with recommendations in the Guide for the Care and Use of Laboratory Animals, prepared by the Institute on Laboratory Animal Resources, National Research Council (DHHS Publ. NIH 86-23, 1985). The Institutional Animal Use and Care Committee at the Tufts Medical Center, in Boston, MA, approved the animal protocol.

The titanium implants (1.05 mm in diameter and 2 mm in length, Institute Straumann AG, Basel, Switzerland) were machined and the surgery was performed as previously described [13]. Briefly, the implantation sites were prepared on the anterior-distal surface of the femurs. After sequential drilling under cooled sterile saline irrigation with 0.4-, 0.5-, 0.7- and 1.0 mm surgical stainless steel twist drills, 3 μl of pBABE or pBABE-SATB2 viral stocks were applied to the bone defects, and the machine-surfaced implants were press-fitted into the slightly undersized holes. For another two groups of TVA mice, 3 μl of RCAS or RCAS-SATB2 viral stocks were applied, and the SLA-surfaced implants were inserted into

the bone defects. The muscles were carefully sutured to cover and stabilize the implants, and the mice were sacrificed 1 and 3 weeks after surgery.

2.4 Histomorphometric Analysis

After euthanasia, the femurs with the implants were isolated, and fixed in 10% neutral-buffered formalin solution. After decalcification, the implants were gently removed, and the femoral tissues were dehydrated, cleared and embedded in paraffin. Tissue sections, 6 μm in thickness, were mounted on glass slides and subjected to H&E staining. Images were taken under a Nikon Eclipse E600 microscope, and the newly formed bone area, which was restricted to the 0.5mm area surrounding the implant, was measured with Spot Advanced Software (Diagnostic Instruments, Sterling Heights, MI, USA). The percentage of new bone edges in direct contact with the implant surface was also determined [13].

2.5 Immuohistochemical (IHC) staining

IHC staining was performed to detect the expression of BSP using the Histostain-SPKit (AEC, Broad Spectrum. Invitrogen Carlsbad, CA). The primary antibody for BSP (a gift from Dr. Larry Fisher, NIH/NIDCR) was used at a 1:200 dilution following the protocol. The slides were observed under the Nikon Eclipse E600 microscope, and cell counts were performed in the newly formed bone area, which was restricted to the 0.5mm area surrounding the implant. The number of BSP-positive cells was normalized to the total number of cells in the newly formed bone area.

2.6 Real-time RT-PCR analysis

The overlying soft tissues were carefully removed, and the femoral bone tissues bordering the implant (1 mm mesial and distal to the implantation site) were dissected, snap-frozen in liquid nitrogen, and the implant was carefully removed. Total RNA was extracted from the bone tissues with TRIzol reagent (Invitrogen, Carlsbad, CA, USA), and the first strand cDNA was generated with SuperScript III reverse transcriptase (Invitrogen, Carlsbad, CA) and oligo $(dT)_{20}$ primer (Invitrogen, Carlsbad, CA). Real-time reverse transcription-PCR (qRT-PCR) analysis was performed using iQ™ SYBR Green Supermix (Bio-Rad Laboratories, Hercules, CA, USA) on a Bio-Rad iQ5 thermal cycler. The sequences of the primers for amplication of mouse Osx, Runx2, BSP, OC, COLI, and GAPDH are listed in Table 1.

2.7 MicroCT Scanning

After euthanasia, the femurs with the implants were separated, fixed in 10% neutral-buffered formalin solution overnight, kept in 70% ethanol, and scanned with a high-resolution microcomputed tomography (μCT) (CT40; Scanco Medical, Basserdorf, Switzerland). According to the histomorphometric measurements on the H&E stained sections, the newly formed bone was restricted to a 0.5mm area surrounding the implant. Thus, at a 3D level the Hounsfield Unit (HU) of this newly formed bone area was determined using eFilm Workstation 2.12 (Merge Technologies Inc., Milwaukee, WI) as we reported previously [13].

2.8 Statistical Analysis

All results are expressed as means ± SEM of 3 or more independent experiments. One-way ANOVA was used to test significance using the software package origin 8 (Origin lab, Northampton, MA, USA). Values of $p<0.05$ were considered statistically significant.

3. Results

3.1 Histological analysis of bone regeneration

In both pBABE-*Satb2* group and pBABE-hygro group, newly formed bone could be observed 1 week after implantation, and osseointegration was initiated on the bone-implant interface at this time point (Figure 1a, 1b). However, although at this time point no difference was detected in the percentage of bone-to-implant contact between these two groups, the pBABE-*Satb2* group showed a 27% increase in the newly formed bone area when compared with the pBABE-hygro group (Figure 1c). Three weeks after the implantation, the implants were successfully integrated with the host bone in both the pBABE-*Satb2* group and the pBABE-hygro group, and the newly formed woven bone observed 1 week after the surgery was replaced by better-organized lamellar bone (Figure 1d, 1e). Histomorphometric analysis showed that both the newly formed bone area and the percentage of bone-to-implant contact were increased by 60% in the pBABE-Satb2 group when compared with those in the pBABE-hygro group (Figure 1f). Similarly, 1 week after implantation, overexpression of SATB2 in the BSP-expressing bone-forming cells via infection with RCAS-*Satb2* resulted in a twofold increase in the percentage of bone-to-implant contact when compared with the RCAS group (Figure 2c). Three weeks after implantation, the newly formed bone area and bone-to-implant contact was increased by 39% and 42%, respectively, in the RCAS-*Satb2* group when compared with those in the RCAS group.

3.2 Immunohistochemical staining results

IHC staining was performed to evaluate the expression of BSP protein in the newly formed bone area as a marker for osteogenic differentiation, and BSP positive cells were counted for quantitative analysis. We observed more intense BSP signals in the pBABE-*Satb2* group than in pBABE-hygro group at both time points (Figure 3a, 3b, 3d, 3e), and cell counting analysis further indicated increased BSP-positive cells in pBABE-*Satb2* group at both time points (Figure 3c, 3f). Infection with RCAS-*Satb2* also induced an 18% increase in the number of BSP-positive cells 1 week after implantation when compared with the RCAS group (Figure 4c). However, there was no significant difference in the number of BSP-positive cells between the RCAS-*Satb2* group and RCAS group at the later time point (Figure 4f).

3.3 Expression of potent osteogenic transcription factors and bone matrix proteins

To investigate the *in vivo* function of SATB2 in osteogenic differentiation, real-time reverse transcription-PCR (qRT-PCR) analysis was performed using the newly formed bone tissues. We found that the expression levels of SATB2, Osx, Runx2, BSP, and COLI were all significantly higher in the pBABE-*Satb2* group than those in the pBABE-hygro group 1 week after implantation (Figure 5a). However, no significant difference in the OC mRNA level was detected between these two groups (Figure 5a). Three weeks after surgery, the expression levels of SATB2, Osx, Runx2, BSP, COLI, and OC were still significantly higher in the pBABE-SATB2 group than those in the pBABE-hygro group (Figure 5b).

Interestingly in the RCAS-*Satb2* group, the expression level of SATB2 showed a 3.3-fold increase when compared with that in the RCAS group 7 days after implantation. Moreover, the RCAS-*Satb2* group displayed dramatic increases in expression levels of OSX, Runx2, BSP, COLI, and OC, which ranged from 6.14-fold to 16.88-fold, when compared with the RCAS group (Figure 5c). However, 3 weeks after the implantation, no significant difference in the expression levels of SATB2, Osx, Runx2, BSP, COLI, or OC could be detected between RCAS-*Satb2* group and the RCAS group (Figure 5d).

3.4 MicroCT results

MicroCT analysis (Figure 6) showed that 21 days after insertion, the implants were surrounded with newly formed bone and successfully anchored with the host bone in pBABE-*Satb2*, pBABE-hygro, RCAS, and RCAS-*Satb2* group (Figure 6a, 6b, 6d, 6e). Figure 6c and 6f demonstrated that Satb2 markedly enhanced the density of the newly formed bone around the implants.

4. Discussion

In attempt to develop new strategies to accelerate the establishment of osseointegration after dental implantation we performed this study, in which, a potent osteogenic transcription factor, SATB2, was introduced to the implantation sites and was evaluated for its potential to be used as a bioactive molecule to promote bone-to-implant contact. As a nuclear matrix protein, SATB2 positively regulates expressions of multiple osteoblast-specific genes and plays an important role in craniofacial patterning and bone development, making it a plausible candidate gene for bone tissue engineering. Acting as a “molecular node” in a transcriptional network through regulating bone development and osteoblast differentiation, SATB2 interacts with and enhances the transcriptional activity of Runx2 and ATF4, two transcription factors that play essential roles in inducing osteogenic differentiation [14].

In our study, two different viral systems, a retroviral pBABE-hygro system and an avian RCAS viral system, were used to achieve SATB2 over-expression in the implantation sites. The recipient mice of both viral systems, BSP/TVA mice, provide an excellent *in vivo* model for bone regeneration study based on the fact that in these mice, the retroviral receptor, TVA, was driven by a BSP promoter and was selectively expressed in BSP-expressing bone-forming cells. In this system, only these BSP-expressing osteogenic lineage cells can be infected by the replication-competent, subgroup A avian leucosis viral (ASLV) vector, RCAS viral system. In contrast, the pBABE retroviral system, once packaged by pCL-Eco, is able to infect all of the murine cells including all adult stem cells and osteogenic lineage cells.

Consistent with previous findings, we found that SATB2 overexpression, achieved either in all of the local cells via the pBABE retroviral system or only in BSP-expressing cells via the RCAS viral system, resulted in increased new bone formation and enhanced bone-to-implant contact. In addition, after the local administration of SATB2 viral stocks (both pBABE-*Satb2* and RCAS-*Satb2*), expression levels of osteogenic transcription factors and bone matrix proteins were all significantly elevated. Interestingly, we found that at an earlier time point (1 week) after implantation, SATB2 overexpression achieved only in BSP-expressing cells (RCAS-*Satb2* group) induced a 2-fold increase in the percentage of bone-to-implant contact when compared with the control group (RCAS group). In contrast, SATB2 overexpression in all local cells (pBABE-*Satb2* group) only resulted in a 60% increase in the percentage of bone-to-implant contact. However, although 3 weeks after implantation, increased new bone area and elevated percentage of bone-to-implant contact could still be observed in the RCAS-*Satb2* group when compared with those in the RCAS group, these changes were less prominent when compared with the changes observed between the pBABE-*Satb2* group and pBABE-hygro group. In the implantation sites where the RCAS-*Satb2* was applied, only BSP-expressing cells were infected and overexpressed SATB2. These cells had already committed to the osteoblastic lineage, and thus lost the ability of self-renewal and proliferation. In contrast, pBABE-*Satb2* could infect all local cells including adult stem cells with the ability of self-renewal and multi-potential of differentiation, which may prolong and enlarge the effect of the original SATB2 infection until a later time point.

Using IHC staining and cell counting, we observed that the numbers of BSP-positive cells in the pBABE-*Satb2* group were increased by 28% and 40%, respectively, at 1 week and 3 weeks after the surgery when compared with the pBABE-hygro group. In contrast, only an 18% increase in the number of BSP-positive cells was observed in the RCAS-*Satb2* group at 1 week after surgery when compared with the RCAS group, while no significant difference in the number of BSP-positive cells was observed between the RCAS-*Satb2* group and the RCAS group at 3 weeks after surgery. These findings provided another piece of evidence indicating that the RCAS viral system, when used in our BSP/TVA transgenic mice, functions in a relatively shorter time period based on the fact that this viral system could only infect osteoblastic lineage cells.

Although the RCAS viral system was found to function in a relatively shorter time period, it also proved to be a useful model which enabled us to specifically target gene overexpression in the bone tissues. In our study, RCAS-*Satb2* group showed dramatic increases in mRNA levels of SATB2, Osx, Runx2, BSP, COLI, and OC at 1 week after implantation when compared with the RCAS group. In contrast, only moderate changes in mRNA levels of these genes were observed between the pBABE-*Satb2* group and the pBABE-hygro group.

5. Conclusion

Local administration of SATB2 significantly enhances expression levels of osteogenic transcription factors and bone matrix proteins, which consequently accelerates new bone formation around the implantation site and enhances the osseointegration of the dental implant.

Acknowledgments

We appreciate the technical supports from Nicholas Brady for microCT scanning and data analysis, Jamie Chipman and Terri Naumes for animal caring. This work was supported by the combination of International Team of Implantology (ITI) and NIH DE16710 to J. Chen, National Nature Science Foundation of China (81070835) to P.S Yang.

References

1. Linder L, Albrektsson T, Branemark PI, Hansson HA, Ivarsson B, Jonsson U, et al. Electron microscopic analysis of the bone-titanium interface. Acta Orthop Scand. 1983; 54:45–52. [PubMed: 6829281]
2. Branemark PI. Osseointegration and its experimental background. J Prosthet Dent. 1983; 50:399–410. [PubMed: 6352924]
3. Sisti KE, Garcia IR Jr, Guastaldi AC, Antoniolli AC, Rossi R, Brochado Neto Ade L. Analysis of titanium surface irradiated with laser, with and without deposited of durapatite. Acta Cir Bras. 2006; 21 (Suppl 4):57–62. [PubMed: 17293968]
4. Traini TMC, Sammons RL, Mangano F, Macchi A, Piattelli A. Direct laser metal sintering as a new approach to fabrication of an isoelastic functionally graded material for manufacture of porous titanium dental implants. Dent Mater. 2008; 24:1525–1533. [PubMed: 18502498]
5. Faeda RS, Tavares HS, Sartori R, Guastaldi AC, Marcantonio E Jr. Evaluation of titanium implants with surface modification by laser beam. Biomechanical study in rabbit tibias. Braz Oral Res. 2009; 23:137–143. [PubMed: 19684947]
6. Rupp F, Scheideler L, Olshanska N, de Wild M, Wieland M, Geis-Gerstorfer J. Enhancing surface free energy and hydrophilicity through chemical modification of microstructured titanium implant surfaces. J Biomed Mater Res A. 2006; 76:323–334. [PubMed: 16270344]
7. Fuerst G, Gruber R, Tangl S, Sanroman F, Watzek G. Enhanced bone-to-implant contact by platelet-released growth factors in mandibular cortical bone: a histomorphometric study in minipigs. Int J Oral Maxillofac Implants. 2003; 18:685–690. [PubMed: 14579956]

8. Lamberg A, Schmidmaier G, Soballe K, Elmengaard B. Locally delivered TGF-beta1 and IGF-1 enhance the fixation of titanium implants: a study in dogs. Acta Orthop. 2006; 77:799–805. [PubMed: 17068714]

9. Decker JF, Lee J, Cortella CA, Polimeni G, Rohrer MD, Wozney JM, et al. Evaluation of Implants Coated With Recombinant Human Bone Morphogenetic Protein-2 (rhBMP-2) and Vacuum-Dried Using the Critical-Size Supraalveolar Peri-Implant Defect Model in Dogs. J Periodontol. 2010

10. Qi MC, Zhou XQ, Hu J, Du ZJ, Yang JH, Liu M, et al. Oestrogen replacement therapy promotes bone healing around dental implants in osteoporotic rats. Int J Oral Maxillofac Surg. 2004; 33:279–285. [PubMed: 15287312]

11. Duarte PM, Cesar-Neto JB, Sallum AW, Sallum EA, Nociti FH Jr. Effect of estrogen and calcitonin therapies on bone density in a lateral area adjacent to implants placed in the tibiae of ovariectomized rats. J Periodontol. 2003; 74:1618–1624. [PubMed: 14682658]

12. Gabet Y, Muller R, Levy J, Dimarchi R, Chorev M, Bab I, et al. Parathyroid hormone 1–34 enhances titanium implant anchorage in low-density trabecular bone: a correlative microcomputed tomographic and biomechanical analysis. Bone. 2006; 39:276–282. [PubMed: 16617039]

13. Xu B, Zhang J, Brewer E, Tu Q, Yu L, Tang J, et al. Osterix enhances BMSC-associated osseointegration of implants. J Dent Res. 2009; 88:1003–1007. [PubMed: 19828887]

14. Dobreva G, Chahrour M, Dautzenberg M, Chirivella L, Kanzler B, Farinas I, et al. SATB2 is a multifunctional determinant of craniofacial patterning and osteoblast differentiation. Cell. 2006; 125:971–986. [PubMed: 16751105]

15. Dobreva G, Dambacher J, Grosschedl R. SUMO modification of a novel MAR-binding protein, SATB2, modulates immunoglobulin mu gene expression. Genes Dev. 2003; 17:3048–3061. [PubMed: 14701874]

16. Britanova O, Depew MJ, Schwark M, Thomas BL, Miletich I, Sharpe P, et al. Satb2 haploinsufficiency phenocopies 2q32-q33 deletions, whereas loss suggests a fundamental role in the coordination of jaw development. Am J Hum Genet. 2006; 79:668–678. [PubMed: 16960803]

17. Savarese F, Davila A, Nechanitzky R, De La Rosa-Velazquez I, Pereira CF, Engelke R, et al. Satb1 and Satb2 regulate embryonic stem cell differentiation and Nanog expression. Genes Dev. 2009; 23:2625–2638. [PubMed: 19933152]

18. Tu Q, Valverde P, Chen J. Osterix enhances proliferation and osteogenic potential of bone marrow stromal cells. Biochem Biophys Res Commun. 2006; 341:1257–1265. [PubMed: 16466699]

19. Li L, Zhu J, Tu Q, Yamauchi M, Sodek J, Karsenty G, et al. An in vivo model to study osteogenic gene regulation: targeting an avian retroviral receptor (TVA) to bone with the bone sialoprotein (BSP) promoter. J Bone Miner Res. 2005; 20:1403–1413. [PubMed: 16007338]

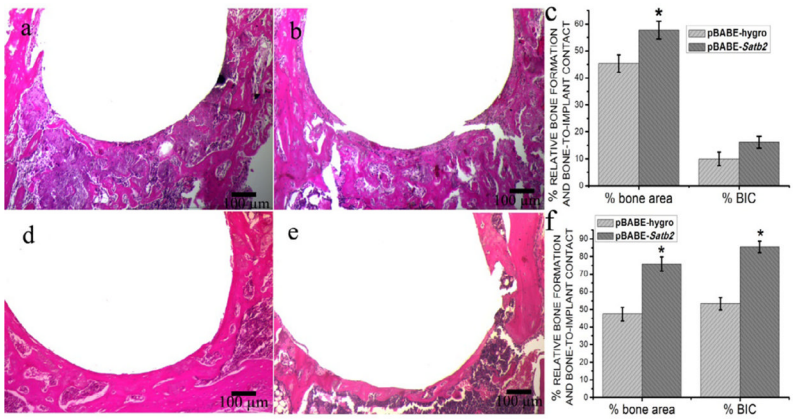

Figure 1. Histomorphometric analysis of pBABE-hygro group and pBABE-*Satb2* group

The photomicrograph of H&E stained tissue sections of pBABE-Satb2 group (a) and pBABE-hygro group (b) 1 week after the implantation showed that newly formed bone could be observed 7 days after implantation, and activated cells were well organized around the implants. The pBABE-*Satb2* group showed a 27% increase in the newly formed bone area when compared with the pBABE-hygro group (c). The photomicrograph of H&E stained tissue sections of pBABE-Satb2 group (d) and pBABE-hygro group (e) 3 weeks after implantation showed that woven bone was replaced by better organized lamellar bone. Histomorphometric analysis showed that both the newly formed bone area and the percentage of bone-to-implant contact were increase by 60% in the pBABE-Satb2 group when compared with those in the pBABE-hygro group (f). Data were expressed as mean ±SEM (n=6–8). **p*<0.05, pBABE-hygro vs. pBABE-*Satb2*.

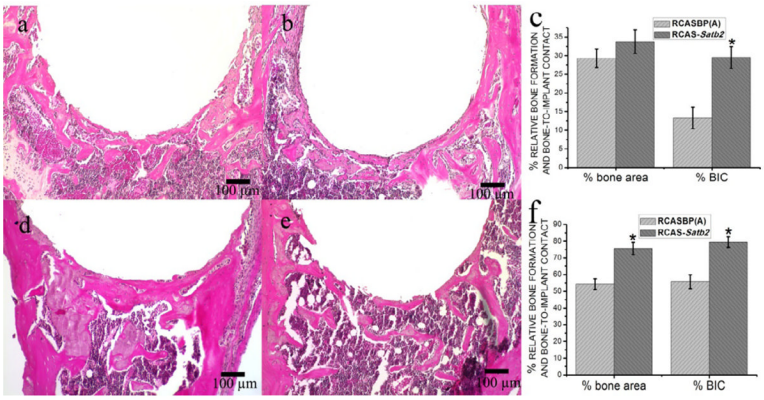

Figure 2. Histomorphometric analysis of RCASBP(A) group and RCAS-*Satb2* group

The photomicrograph of H&E stained tissue sections of RCAS-Satb2 group (a) and RCAS group (b) 1 week after the implantation showed similar results in the pBABE-hygro and pBABE-Satb2 group. Overexpression of Satb2 via infection with RCAS-Satb2 resulted in a 2-fold increase in the percentage of bone-to-implant contact when compared with the RCAS group (c).

The representative slides of the H&E staining results of RCAS-Satb2 group (d) and RCAS group (e) showed similar results as in Figure 1d and 1e. The percentage of bone formation surrounding the implant and the percentage of bone-in-contact with host bone were determined at day 7 and 21 post operation (f). Data were expressed as mean±SEM (n=6–8). *p<0.05, RCAS vs. RCAS-*Satb2*.

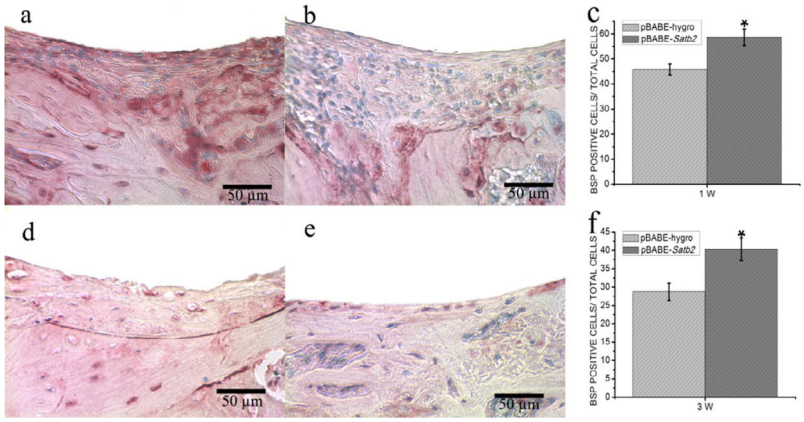

Figure 3. Immunohistochemical analysis of pBABE-Satb2 group and pBABE-hygro group

(a–b) Immunohistochemical staining for BSP showed that there were more intense BSP signals in the pBABE-Satb2 group (a) than that in pBABE-hygro group (b) 1 week after implantation. (c) BSP positive cell counting analysis indicated increased BSP-positive cells in pBABE-Satb2 group than that in pBABE-hygro group. (d–e) Representative pictures of (d) pBABE-Satb2 group and (e) pBABE-hygro group 3 weeks after operation. (f) Cell counting demonstrated that there were more BSP-positive cells in pBABE-Satb2 group than that in pBABE-hygro group. Data were expressed as mean±SEM (n=6–8). *$p<0.05$, pBABE-hygro vs. pBABE-*Satb2*.

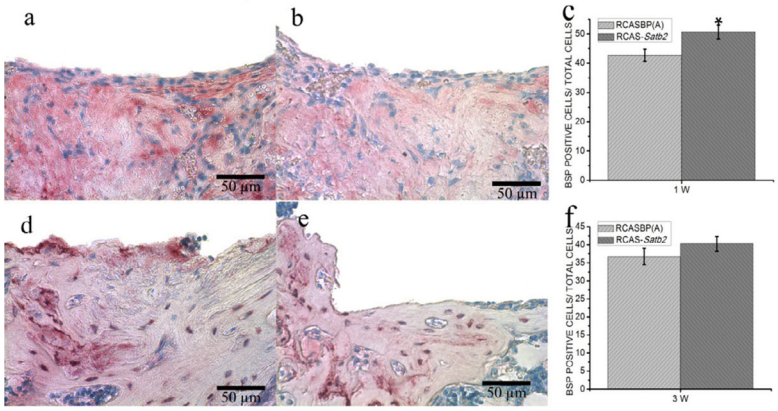

Figure 4. Immunohistochemical analysis of RCASBP(A) group and RCAS-*Satb2* group

(a–b) Immunohistochemical staining for BSP fromRCAS-Satb2 group (a) and RCAS group (b) 1 week after implantation. (c) BSP positive cell counting analysis indicated increased BSP-positive cells in RCAS-Satb2 group than that in RCAS group. (d–e) Representative pictures of IHC staining results from (d) RCAS-Satb2 group and (e) RCAS group 3 weeks after operation. (f) Cell counting demonstrated that there were more BSP-positive cells in RCAS-Satb2 group than that in RCAS group. Data were expressed as mean±SEM (n=6–8). Data were expressed as mean±SEM (n=6–8). *p<0.05, RCAS vs. RCAS-*Satb2*.

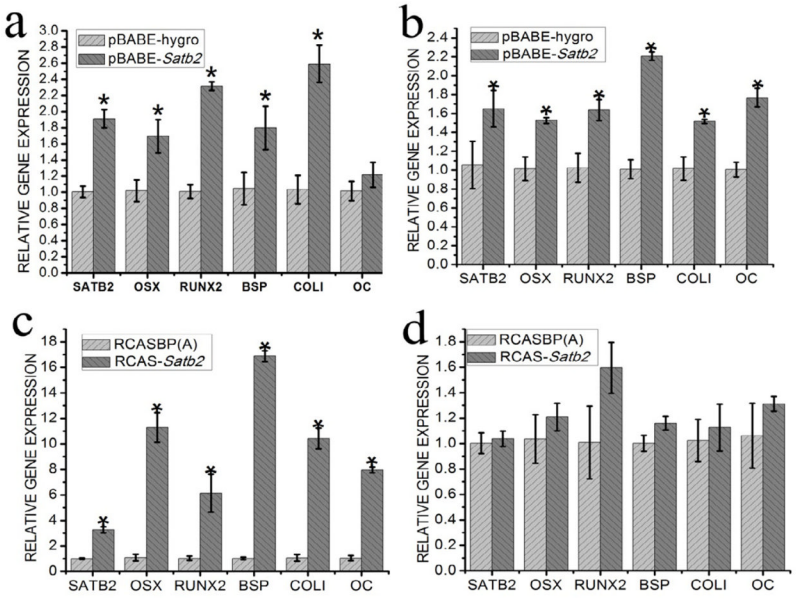

Figure 5. Overexpression of SATB2 enhances expression levels of potent osteogenic transcription factors and bone matrix proteins

To investigate the *in vivo* function of SATB2 in osteogenic differentiation, qRT-PCR analysis was performed to detect the expression levels of SATB2, Osx, Runx2, BSP, COLI and OC in the newly formed bone tissues. (a)Gene expression in pBABE-Satb2 group and pBABE-hygro group1 week after implantation; (b) Gene expression in pBABE-Satb2 group and pBABE-hygro group3 week after implantation; (c)Gene expression in RCASBP(A) group and RCAS-*Satb2* group 1 week after operation; (d) Gene expression in RCASBP(A) group and RCAS-*Satb2* group 3 week after operation. Data were expressed as mean±SEM (n=3). **p*<0.05.

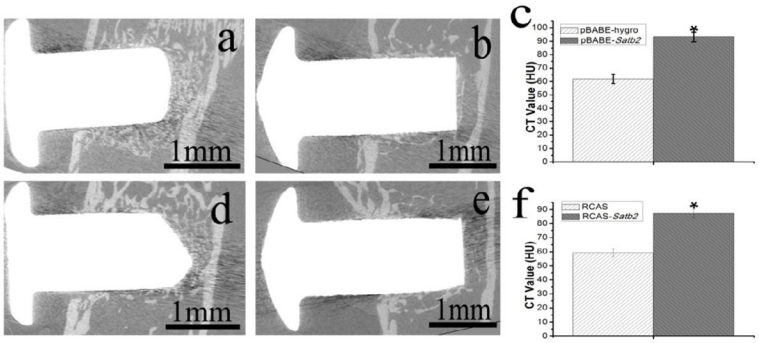

Figure 6. MicroCT analysis indicated that

, 21 days after insertion, the implants were surrounded with newly formed bone and successfully anchored in the host bone in (a) pBABE-*Satb2*, (b) pBABE-hygro, (d) RCAS-*Satb2* and (e) RCAS group. (c) The CT value of the newly formed bone surrounding the implant was higher in pBABE-SATB2 group than that in pBABE-hygro group. (f) And similar results can be found in RCAS-Satb2 group than RCAS group. Data were expressed as mean±SEM (n=3–6). **p*<0.05.

TABLE 1

The sequences of the primers for qRT-PCR in the experiment.

Primer	Sequence
SATB2	forward : 5’-GCCGTGGGAGGTTTGATGATT-3'
	reverse : 5’-ACCAAGACGAACTCAGCGTG-3'
OSX	forward: 5'-ATGGCGTCCTCTCTGCTTG-3'
	reverse: 5'-TGAAAGGTCAGCGTATGGCTT-3'
RUNX2	forward : 5’-CCCAGCCACCTTTACCTACA-3'
	reverse : 5’-TATGGAGTGCTGCTGGTCTG -3'
BSP	forward: 5'-CAGGGAGGCAGTGACTCTTC-3'
	reverse: 5'-AGTGTGGAAAGTGTGGCGTT-3'
COLI	forward: 5'-TGACTGGAAGAGCGGAGAGT-3'
	reverse: 5'-GTTCGGGCTGATGTACCAGT-3'
OCN	forward : 5'-GCGCTCTGTCTCTCTGACCT-3'
	reverse : 5'-GCCGGAGTCTGTTCACTACC-3'
GAPDH	forward: 5'-AGGTCGGTGTGAACGGATTTG-3'
	reverse: 5'-TGTAGACCATGTAGTTGAGGTCA-3'